Optical conductivity of charge carriers interacting with a two-level systems reservoir

A. Villares Ferrer
Instituto de Física, Universidade Federal Fluminense, Av. Gral Milton Tavares de Souza s/n, Niterói 24210-346, Rio de Janeiro, Brazil

A. O. Caldeira
Instituto de Física "Gleb Wataghin," Departamento de Física da Matéria Condensada, Universidade Estadual de Campinas, Caixa Postale 6165, Campinas 13083-970, São Paulo, Brazil

C. Morais Smith
Institute for Theoretical Physics, University of Utrecht, Leuvenlaan 4, 3584 CE, Utrecht, The Netherlands
(Received 5 May 2006; published 9 November 2006)

Using the functional-integral method we investigate the effective dynamics of a charged particle coupled to a set of two-level systems as a function of temperature and external electric field. The optical conductivity and the direct current (dc) resistivity induced by the reservoir are computed. Three different regimes are found depending on the two-level system spectral function, which may lead to a non-Drude optical conductivity in a certain range of parameters. Our results contrast to the behavior found when considering the usual bath of harmonic oscillators which we are able to recover in the limit of very low temperatures.

DOI: 10.1103/PhysRevB.74.184304 PACS number(s): 73.21.−b, 73.43.Lp

I. INTRODUCTION

The possibility of manipulating physical systems at length scales where quantum effects become important has attracted much attention over the last years. This scenario has stimulated considerable effort in the study of quantum open systems, first because of its relevance to the phenomenon of quantum coherence and second because it might not be entirely obvious the way in which we can obtain information about the quantum dynamics of the system of interest coupled to its environment. One of the strategies broadly used in solving this problem consists in the replacement of the environment by an approximate model. This must be done in such a way that after tracing the environment coordinates out, the problem can be formulated only in terms of the variables of the system of interest.[1] It is remarkable that most of the environments can be represented either in terms of a bath of oscillators,[2,3] when the physics is dominated by the delocalized modes, or by an spin bath,[4] when the localized modes play the major role. In this paper we will be interested in another type of thermal bath that can be thought of as the projection of the usual oscillator modes onto their two lowest lying levels. At very low temperatures, these truncated two-level systems (TLSs) have the same properties as the usual harmonic oscillators, that is, the two baths exhibit the same quantum limit. However, as we will show, they strongly differ in the classical regime, at high temperatures.

It is now well known that when the oscillator model with linear spectral density is used to mimic a thermal bath interacting with a quantum particle, the wave packet associated with the latter undergoes a damped motion, exactly as in the classical problem.[2] In this situation, and within the long time approximation, the average over the environment variables results in an equation of motion for the particle without memory effects. Therefore, it directly follows that the transport properties of the quantum particle can be simply described in terms of the damping and diffusion coefficients. As a consequence, the optical conductivity $\sigma(\omega)$ of a single particle coupled to an oscillator bath has, in the so-called ohmic case, only an incoherent part, which has a Drude-like form. In this case the Lorentzian width is determined by a *temperature independent* damping constant.

The phenomenological approach of representing the environment by an oscillator bath was successfully used in the study of dissipative effects in macroscopic quantum coherence[3] (the spin-boson model) and macroscopic quantum tunneling.[5] Moreover, there are particular situations, see Ref. 6 for instance, in which the oscillator model can be derived from microscopic theories just following the prescriptions of Feynman and Vernon.[1] That is also the case of solitons, whose transport properties can be investigated using the collective coordinate quantization scheme.[7–9] In those cases the effective equation of motion for the center of mass of the soliton leads, in the long time regime, to a *temperature dependent* damping constant. The form of the damping constant is such that the optical conductivity of a system of noninteracting solitons has again a Drude-like form, and in the low temperature limit correctly reproduces the finite free particle Drude weight at zero frequency. This behavior is completely general for solitons and therefore independent of the nonlinear field theory that supports these localized solutions. From Refs. 2 and 7–9 we can conclude that, within the long time regime, the optical properties of quasiparticles coupled to an oscillator bath have always the trivial Drude form. Therefore, if results obtained from measurements of $\sigma(\omega)$ are at variance with the latter, they cannot be attributed solely to the above-mentioned particle-reservoir interaction. In those cases more complicated models are required[10] or alternative thermal bath descriptions should be employed.[4]

In this paper, our main goal is to present a different kind of thermal reservoir which, in addition to a dissipative dynamics for the charge carriers, induces a nontrivial optical conductivity. Our starting point will be the problem of a single particle subject to a complex potential which can be

represented as a distribution of local two-level systems. Using the well known Feynman-Vernon formalism[1] we are able to traced out the environment modes and obtain the reduced density operator of the particles. This operator will be expressed in terms of an effective action containing all the information about the coupling of the carriers to the reservoir and provides us with an equation of motion for the particles from which the transport properties can be computed. In this way it will be shown that the optical conductivity of this system has a temperature dependent non-Drude behavior with a very rich structure which contrasts with the oscillator bath transport properties.

This paper will be divided as follows. In Sec. II we present a model describing a single particle interacting with a set of TLSs. In Sec. III an effective equation of motion describing the particle dynamics will be derived and in Sec. IV the optical conductivity of the system is calculated considering different characteristics of the thermal reservoir. Finally, in Sec. V, we discuss our results and present the conclusions.

II. THE MODEL

As it was already mentioned, we will be interested in the transport properties of a single particle coupled to a generic TLSs reservoir. This problem can be completely described by the Hamiltonian

$$H = H_0 + H_r + H_i, \tag{1}$$

where H_0 stands for a particle placed in an external electric field, and it is given by

$$H_0 = \frac{\hat{p}^2}{2M} + exE. \tag{2}$$

The distribution of TLSs playing the role of thermal reservoir in Eq. (1) is denoted by H_r and may be expressed in the k space as

$$H_r = \sum_{k=1}^{N} \frac{\hbar\omega_k}{2}\sigma_{zk}, \tag{3}$$

where σ_{zk} is the z Pauli matrix. Finally, the interaction H_i between the particle of interest and the thermal bath will be taken in such a way to induce transitions between the states of each TLS. A suitable choice is

$$H_i = -x\sum_{k=1}^{N} J_k\sigma_{xk}, \tag{4}$$

where J_k and σ_{xk} are, respectively, the coupling constant and the x Pauli matrix.

Although the problem defined by Eqs. (1)–(4) was not derived from a microscopic description of a concrete physical system, it is still very useful because there are many systems which, under certain circumstances, behave as a truncated TLS. Indeed, in the process of modeling defects in crystalline solids or amorphous materials, one has to deal with a distribution of locally quadratic-plus-quartic potentials, as it is shown in Fig. 1. In fact, if each local double well in the distribution has fairly separated minima, and the typical energy scale $\hbar\omega_c$ (obtained by the harmonic approximation about each minimum and assuming they do not differ much) is such that $\hbar\omega_c \gg kT$ (see Refs. 3 and 11 for details), all the locally quartic potentials at positions l can be effectively described as two-level systems and

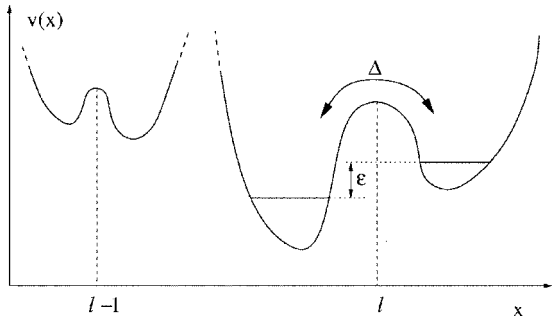

FIG. 1. Complex potential with multiple local quartic structure. The effective TLS at site l is described in terms of the detuning ε between the wells ground states and a typical matrix element for the tunneling processes Δ.

$$H_l = -\frac{1}{2}(\Delta_l\sigma_{xl} - \varepsilon_l\sigma_{zl}), \tag{5}$$

where Δ_l is a typical matrix element for the tunneling process between the two minima and ε_l is the "detuning" between the ground states in the two wells. This fact suggests a possible phenomenological description for a particle moving in a complex potential as shown in Fig. 1, where the source of dissipation is the induced transition between the states of the TLSs ensemble and may have the form (4). However, in the course of this procedure one should keep in mind that although the rate ε_l/kT may have any value, the TLSs representation is valid only if $\hbar\omega_c \gg kT \sim (\hbar\Delta_l, \varepsilon_l)$. Therefore the high temperature limit should be understood as $\hbar\omega_c \gg kT > \hbar\Omega$, where Ω is the cutoff frequency of the system, which can be assumed to be of the order of max $(\hbar\Delta_l, \varepsilon_l)$. In other words, we are saying that the TLSs description is only valid for intermediate temperatures since extreme cases will, in this particular example, reproduce the well-known results of the bath of oscillators.

Now, knowing the details of the coupling of the external particle to the TLSs array we can perform the Fourier transform to k space and reach a Hamiltonian whose main physical effects can be mimicked by Eq. (1).

If the reader is still uneasy about the way we obtained the TLS bath he or she is urged to see a more thorough analysis of this issue in Ref. 4.

III. EFFECTIVE PARTICLE DYNAMICS

This section is devoted to investigating the effective dynamics of a particle interacting with the TLS thermal reservoir. We will use the Feynman-Vernon functional integral approach, which begins with the calculation of the reduced density operator of the particle of interest, namely,

$$\rho(x,y,t) = \mathrm{Tr}[\langle x|e^{-iHt/\hbar}\rho(0)e^{iHt/\hbar}|y\rangle], \tag{6}$$

where we are using the coordinate representation for the particle states, Tr denotes the trace over the bath modes, and H is the Hamiltonian of the total system given by Eq. (1).

The density operator of the whole system at time $t=0$ will be assumed to be separable, $\rho(0)=\rho_p(0)\rho_r(0)$, where p and r denote the particle and the reservoir, respectively. The reduced density operator (6) can be written as

$$\rho(x,y,t) = \int dx' \int dy' \rho_p(x',y',0)\mathcal{J}(x,y,t;x'y',0),$$

where the superpropagator $\mathcal{J}$ has the form

$$\mathcal{J} = \int_{x'}^{x} \mathcal{D}x(t') \int_{y'}^{y} \mathcal{D}y(t') e^{(i/\hbar)(S_0[x]-S_0[y])} \mathcal{F}[x,y]. \tag{7}$$

In the expression above

$$S_0[z] = \int_0^t \left[\frac{M}{2}\dot{z}^2(t') + ez(t')E(t') \right] dt'$$

corresponds to the action of a free particle in the presence of an electric field and $\mathcal{F}$ denotes the influence functional, which is given by

$$\mathcal{F}[x,y] = \mathrm{Tr}\left[\rho_r(0) \left(T \exp \frac{i}{\hbar} \int_{t_0}^{t} \tilde{H}_i(y(t'))dt' \right) \times \left(T \exp -\frac{i}{\hbar} \int_{t_0}^{t} \tilde{H}_i(x(t'))dt' \right) \right], \tag{8}$$

where T indicates time-ordered product and

$$\tilde{H}_i(z) = e^{(i/\hbar)H_r t} H_i(z(t')) e^{-(i/\hbar)H_r t}.$$

The central quantity in this method is the influence functional defined in Eq. (7). Our next step is to derive an explicit expression for it. Although this quantity has already been evaluated through different approaches for interactions of the form (4),[12] here we will sketch its derivation for the sake of completeness.

In order to proceed, we will assume that the interaction strength is weak enough, such that we may expand Eq. (8) in powers of J_k and retain only terms up to second order. We then obtain

$$\mathcal{F}[x,y] = 1 - \frac{1}{\hbar^2} \int_0^t dt' \int_0^{t'} dt'' \{ \langle \tilde{H}_i(x(t'))\tilde{H}_i(x(t'')) \rangle + \langle \tilde{H}_i(y(t''))\tilde{H}_i(y(t')) \rangle - \langle \tilde{H}_i(y(t'))\tilde{H}_i(x(t'')) \rangle - \langle \tilde{H}_i(y(t''))\tilde{H}_i(x(t')) \rangle \}, \tag{9}$$

where the average value of an observable A is given by

$$\langle A \rangle = \left[2^N \prod_{k=1}^{N} \cosh\left(\frac{\hbar\omega_k}{2k_BT} \right) \right]^{-1} \mathrm{Tr}[e^{-H_r/k_BT} A].$$

After tracing the reservoir degrees of freedom from Eq. (9), the influence functional acquires the form

$$\mathcal{F}[x,y] = 1 - \frac{1}{\hbar^2} \int_0^t dt' \int_0^{t'} dt'' \sum_{k=1}^{N} J_k^2 \left\{ f(x,y)\cos[\omega_k(t'-t'')] - ig(x,y)\tanh\left(\frac{\hbar\omega_k}{2k_BT} \right) \sin[\omega_k(t'-t'')] \right\}, \tag{10}$$

where

$$f(x,y) = x(t')x(t'') + y(t'')y(t') - y(t')x(t'') - y(t'')x(t'),$$

and

$$g(x,y) = x(t')x(t'') - y(t'')y(t') + y(t')x(t'') - y(t'')x(t').$$

Equation (10) may be simplified by introducing a set of coordinates corresponding to the particle center of mass q and relative coordinate ξ. Therefore, $x=q+\xi/2$, $y=q-\xi/2$, and the influence functional reads

$$\mathcal{F}[x,y] = 1 - \frac{1}{\hbar^2} \int_0^t dt' \int_0^{t'} dt'' \sum_{k=1}^{N} J_k^2 \left\{ \xi(t')\xi(t'')\cos[\omega_k(t'-t'')] - 2iq(t')\xi(t'')\tanh\left(\frac{\hbar\omega_k}{2k_BT} \right) \sin[\omega_k(t'-t'')] \right\}. \tag{11}$$

In the majority of cases considered we do not have enough information about the system which would allow us to perform the above summation in k. In order to overcome this difficulty, one usually introduces a phenomenological spectral density function, which correctly describes the bath in some well-known limit.[2] Because we intend to follow this strategy, we will first calculate the form of the spectral density function associated to the two-level system reservoir and will replace it by some phenomenological guess afterwards.

The spectral function can be obtained from

$$J(\omega) = \mathrm{Im}(\mathfrak{F}\langle -i\Theta(t-t')[F(t),F(t')] \rangle), \tag{12}$$

where $F(t)$ is the force produced by the particle on the thermal bath, $\Theta(t)$ is the usual step function, and $\mathfrak{F}$ stands for the Fourier transform. From Eq. (4) it is straightforward to demonstrate that $F(t)=\Sigma_k J_k \sigma_{xk}$. Substituting then the expression for the force into Eq. (12) and using Eq. (3) we obtain

$$J(\omega,T) = \sum_{k=1}^{N} \pi J_k^2 \tanh\left(\frac{\hbar\omega_k}{2k_BT} \right) \delta(\omega_k - \omega). \tag{13}$$

Notice that the above expression is completely different from the oscillator spectral function. Here, all modes with energy well below k_BT contribute less effectively to the spectral density than the "unoccupied" modes above the thermal energy. Therefore, any attempt to replace Eq. (13) by a phenomenological guess should preserve this property.

If we now replace Eq. (13) into Eq. (11), we obtain the influence functional

$$\mathcal{F} = \exp\left\{ -\frac{1}{\hbar}\int_0^t dt' \int_0^{t'} dt'' \int_0^\infty d\omega \frac{J(\omega,T)}{\pi}\left[\coth\left(\frac{\hbar\omega}{2k_BT}\right)\xi(t')\xi(t'')\cos[\omega(t'-t'')] - 2iq(t')\xi(t'')\sin[\omega(t'-t'')]\right]\right\}, \quad (14)$$

where we have reexponentiated the second order expansion used in Eq. (9).

Next, we substitute Eq. (14) into Eq. (7) to obtain the superpropagator for the particle of interest, namely

$$\mathcal{J} = \int \mathcal{D}\xi \int \mathcal{D}q \exp\left\{\frac{i}{\hbar}S_{eff}[q,\xi]\right\} \times \exp\left\{ -\frac{1}{\hbar}\int_0^t \int_0^{t'} \Phi(t'-t'')\xi(t')\xi(t'')dt'dt''\right\}.$$

In the above equation, the effective action is given by

$$S_{eff} = \int_0^t dt' \left[M\dot{q}(t')\dot{\xi}(t') + e\xi(t')E(t') + \int_0^{t'} \Lambda_1(t'-t'')q(t')\xi(t'')dt''\right], \quad (15)$$

where

$$\Lambda_1 = \frac{2}{\pi}\int_0^\infty J(\omega,T)\sin[\omega(t'-t'')]d\omega$$

and

$$\Phi = \frac{1}{\pi}\int_0^\infty J(\omega,T)\cos[\omega(t'-t'')]\coth\left(\frac{\hbar\omega}{2k_BT}\right)d\omega.$$

After having traced the environment coordinates, we can derive from the effective action (15) an equation of motion for the time evolution of the particle center of mass q and for the width ξ of the wave packet associated to it,

$$M\ddot{q}(t) + \int_0^t \Lambda(t-t')\dot{q}(t')dt' = eE(t), \quad (16)$$

$$M\ddot{\xi}(t) + \int_0^t \Lambda(t-t')\dot{\xi}(t')dt' = 0, \quad (17)$$

where we have performed an integration by parts in order to explicitly show the viscous force of the TLSs reservoir acting on the particle and

$$\Lambda(t-t') = \frac{2}{\pi}\int_0^\infty \omega^{-1}J(\omega,T)\cos[\omega(t-t')]d\omega. \quad (18)$$

The last step consists in solving Eqs. (16) and (17). However, we must first specify the form of the spectral density of the bath. Because we intend to keep the problem as general as possible, we will choose a form for the spectral density which retains the functional T dependence given by Eq. (13). We then assume that

$$J(\omega,T) = \frac{\pi}{2}\bar{\gamma}\omega^s \tanh\left(\frac{\hbar\omega}{2k_BT}\right)\Theta(\Omega-\omega), \quad (19)$$

where Ω is the cutoff frequency already introduced in the discussion of the model and $\bar{\gamma}$ is a constant defining the particle coupling strength to the TLSs. The reader must be warned that $\bar{\gamma}$ used in this paper is actually $4\gamma/\pi$, where γ is the usual parameter that appears in the same context for the bath of oscillators. The exponent s in the expression above determines the long time (or low frequency) properties of the thermal bath and its value is chosen to be real and positive. This is a consequence of having assumed that $J(\omega)$ is a smooth function of ω, which up to some cutoff frequency can be represented in a polynomial fashion.[14] The specific value of s is related to the *kind* of dissipation provided by the bath. For instance, in the usual model of the bath of oscillators, $s=1$ characterizes the most common case of ohmic dissipation, implying that the corresponding equation of motion is a Langevin equation containing a dissipative term depending on the velocity whereas for $s=3$ the equation of motion contains a dissipative term depending on the third derivative of the position. This happens for the Abraham-Lorentz equation, which describes an electron interacting with its own radiation field.[15]

Expression (19) retains the main properties of the functional form (13), namely the fact that the temperature determines which are the statistically relevant modes. Therefore, for a given value of Ω and depending on the temperature, the particle may simply have no interaction, on average, with the reservoir. Notice that this choice is at variance with the one employed in Ref. 13 where the author maps the system onto a bath of oscillators.

By replacing Eqs. (18) and (19) into (16), we obtain the following equation for the velocity of the particle center of mass:

$$\dot{v}(t) + \bar{\gamma}\int_0^t \Gamma(t-t')v(t')dt' = \frac{eE(t)}{M}, \quad (20)$$

with the damping function

$$\Gamma(t-t') = \int_0^\Omega \omega^{s-1}\tanh\left(\frac{\hbar\omega}{2k_BT}\right)\cos[\omega(t-t')]d\omega. \quad (21)$$

As it can be observed from Eq. (20), after tracing the two-level system reservoir coordinates, we have obtained an equation of motion for the particle's center of mass in which the thermal bath has the same effect as that of a *viscous fluid*. It should be noticed that for $s=1$ and zero temperature, Eq. (21) reduces to the oscillator-bath damping function, which is memoryless in the limit $\Omega\to\infty$ or, in other words, in the long time regime. Indeed, in this case

$$\Gamma(t-t') = \lim_{\Omega\to\infty} \int_0^{\Omega} \cos(\omega[t-t'])d\omega = \pi\delta(t-t'),$$

indicating that the damping is a purely instantaneous function.

However, if $s \neq 1$ we realize that even at zero temperature and with the cutoff frequency going to infinity, it is impossible to obtain a damping function without memory. In this situation the problem becomes non-Markovian and the particle dynamics cannot be described in terms of damping and diffusion coefficients. In the following, we will investigate the transport properties of a system of noninteracting particles described by Eqs. (20) and (21) through the evaluation of its optical conductivity.

IV. THE OPTICAL CONDUCTIVITY

The current associated to distinguishable noninteracting particles described by the equation of motion (20) reads $j = ev(t)$, where j satisfy

$$\frac{dj}{dt} + \bar{\gamma}\int_0^t \Gamma(t-t')j(t')dt' = \frac{e^2E(t)}{M}. \tag{22}$$

This equation may be solved by the well-known method of the Laplace transform. If we assume that initially there is no current in the system, Eq. (22) may be written as $j(z) = \sigma(z)E(z)$, with

$$\sigma(z) = \frac{e^2}{M[z + \bar{\gamma}\Gamma(z)]},$$

where $\Gamma(z)$ is the Laplace transform of $\Gamma(t-t')$. For all allowed values of s, $\Gamma(z)$ can be written as (see the Appendix)

$$\Gamma(z) = \frac{\Omega^{s+1}F\left(s,-\frac{\Omega^2}{z^2}\right)}{(s+1)z^2}\tan\left(\frac{\hbar z}{2kT}\right) - \frac{4k_BTz\Omega^{s+1}}{\hbar(s+1)}\sum_{n=1}^{\infty}\frac{F\left(s,-\frac{\Omega^2}{\lambda_n{}^2}\right)}{\lambda_n{}^2(\lambda_n^2 - z^2)}, \tag{23}$$

where F denotes hypergeometric functions given by $F(s,x) = {}_2F_1\left(1,\frac{1+s}{2},\frac{3+s}{2},x\right)$ and $\lambda_n = (2n-1)\pi k_BT/\hbar$, with $n \in \mathbb{N}$.

The optical conductivity may now be promptly obtained by substituting Eq. (23) into

$$\sigma(\omega) = \lim_{\delta\to 0^+} \mathrm{Re}\left[\frac{e^2/M}{z + \bar{\gamma}\Gamma(z)}\bigg|_{z=\delta-i\omega}\right]. \tag{24}$$

Although Eqs. (23) and (24) allow us to compute $\sigma(\omega)$ for any $s \geqslant 0$, it may be enlightening to consider the problem for specific values of s, for which the hypergeometric series in Eq. (23) converge to simple functions. In this way we will be able to proceed analytically in the investigation of the optical conductivity and obtain, if there are such contributions, the temperature dependence of the Drude weight and the incoherent conductivity in the whole frequency range. In the following we will focus on particular cases illustrating the superohmic ($s>1$), ohmic ($s=1$), and subohmic ($s<1$) situations.

A. Superohmic case, $s=2$

In this specific case, the hypergeometric functions involved in Eq. (23) acquire a simple form

$${}_2F_1(1,3/2,5/2,-x^2) = \frac{3}{x}\left(\frac{1}{x} - \frac{\arctan x}{x^2}\right),$$

and the Laplace transform of the damping function reduces to

$$\Gamma(z) = \frac{4z}{\pi}\sum_{n=1}^{\infty}\frac{(2n-1)\arctan[\hbar\Omega/\pi k_BT(2n-1)]}{(2n-1)^2 - (\hbar z/\pi k_BT)^2} - z\arctan\left(\frac{\Omega}{z}\right)\tan\left(\frac{\hbar z}{2k_BT}\right). \tag{25}$$

Substituting then Eq. (25) into Eq. (24), we obtain the following form for the optical conductivity:

$$\sigma(\omega) = \sigma^{DW}(T)\,\delta(\omega) + \sigma^{inc}(\omega,T), \tag{26}$$

where $\sigma^{DW}(T)$ represents the Drude weight, whereas $\sigma^{inc}(\omega,T)$ stands for the incoherent contribution. Let us first analyze $\sigma^{DW}(T)$, which is given by

$$\sigma^{DW}(T) = \sigma_0\left[1 + \frac{4\bar{\gamma}}{\pi}\sum_{n=1}^{\infty}\frac{\arctan[\hbar\Omega/\pi k_BT(2n-1)]}{(2n-1)}\right]^{-1}, \tag{27}$$

where $\sigma_0 = \pi e^2/M$ is the Drude weight of the free particle. Although this sum cannot be performed exactly for all temperatures, we may derive an analytical expression for it in the regime $k_BT \gg \hbar\Omega$. We then find

$$\sigma^{DW}(T) = \frac{\sigma_0}{1 + 4\bar{\gamma}\hbar\Omega/\pi^2k_BT\sum_{n=1}^{\infty}1/(2n-1)^2} = \frac{\sigma_0}{(1 + \bar{\gamma}\hbar\Omega/2k_BT)}, \tag{28}$$

where the damping term provides a small correction to the particle mass. Notice that Eq. (28) correctly reproduces the free particle behavior at high temperatures. This result is in agreement with the fact that as the temperature is raised the high frequency TLSs will play a major role in the composition of the spectral function which justifies the mass correction as due to the adiabatic approximation. In other words, the high frequency TLSs adiabatically dress the moving particle.

A numerical evaluation of the sum involved in Eq. (27) yields the general behavior of the Drude weight as a function of temperature [see Fig. 2(a)]. Observe that the conductivity grows with temperature until it saturates at the value of a free particle in the $T\to\infty$ limit. In order to investigate the functional growth of the conductivity with temperature, we have

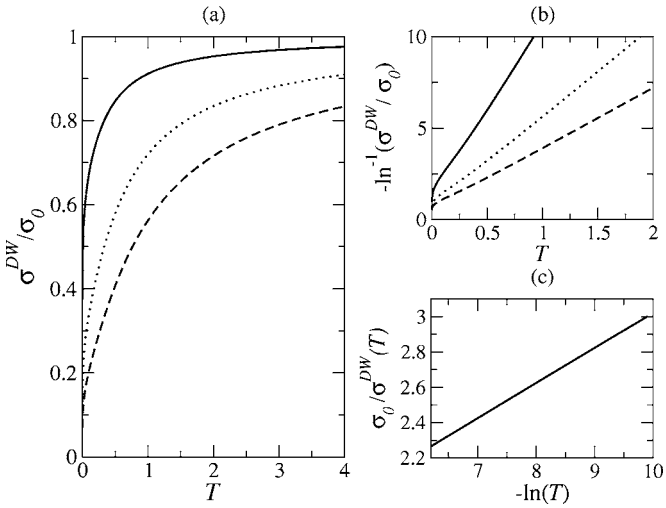

FIG. 2. (a) Drude weight as a function of T for $\Omega=1$, the continuous, dotted, and dashed lines correspond to $\bar{\gamma}=0.2$, $\bar{\gamma}=0.8$, and $\bar{\gamma}=1.6$, respectively. (b) Temperature behavior of $-1/\ln \sigma^{DW}$, the continuous, dotted, and dashed lines correspond to $\bar{\gamma}=0.2$, $\bar{\gamma}=0.4$, and $\bar{\gamma}=0.6$, respectively. (c) $1/\sigma^{DW}$ vs $-\ln T$ for low temperatures and $\bar{\gamma}=0.2$. In all cases it is assumed $\hbar=k_B=1$ and the Drude weight is measured in units of σ_0.

plotted $-1/\ln \sigma^{DW}(T)$ vs T in Fig. 2(b). The plot is linear in T, except in the low temperature region. We may therefore conclude that for high temperatures the Drude weight behaves as $\sigma^{DW} \propto \exp[-1/(\alpha+\beta T)]$, where the constants α and β can be determined from the plots and depend on the values of Ω and $\bar{\gamma}$. On the other hand, the vanishing of $\sigma^{DW}(T)$ as the temperature is lowered was already expected from Eq. (27), because for strictly zero temperature the sum to be performed is positive and divergent.

The functional reduction of the conductivity as the temperature decreases may be determined by considering a certain $\bar{N}=2\bar{n}-1$ such that $\hbar\Omega/\pi k_B T\bar{N} \gg 1$. In the limit of $T \to 0$ the value of $\bar{N}$ will be of the order of $\hbar\Omega/k_B T$. In this situation Eq. (27) may be approximately written as

$$\sigma^{DW}(T) \sim \sigma_0 \left[2\bar{\gamma}\mathcal{S} + \frac{4\bar{\gamma}}{\pi} \sum_{n=\bar{n}}^{\infty} \frac{\arctan[\hbar\Omega/\pi k_B T(2n-1)]}{(2n-1)} \right]^{-1}, \tag{29}$$

where

$$\mathcal{S} = \sum_{n=1}^{\bar{n}} \frac{1}{2n-1} = \alpha + \frac{1}{2}\psi^{(0)}(\bar{n}+1/2), \tag{30}$$

with $\alpha=(C+\ln 4)/2$,

$$C = \lim_{m\to\infty} \sum_{k=1}^{m} \frac{1}{k} - \ln m,$$

and $\psi^{(0)}$ denote the polygamma function of zero order given by $\psi^{(0)}(x)=\partial_x \ln \Gamma(x)$. In the zero temperature limit the sum given by Eq. (30) dominates the behavior of Eq. (29). Using then the Stirling expansion and assuming that $\bar{n}$ is of the order of $\hbar\Omega/k_B T$, we finally obtain that the Drude weight in the low temperature limit behaves as

$$\sigma^{DW}(T \to 0) \sim \frac{e^2}{M[\bar{\gamma}\alpha/\pi + \ln(k_B T/\hbar\Omega)^{-\varepsilon\bar{\gamma}}]}. \tag{31}$$

In the expression above ε is a numerical factor that can be determined from the plot of $1/\sigma^{DW}$ vs $-1/\ln T$ for low temperatures. Inspection of Fig. 2(c) indicates that the value of ε is approximately 1. Therefore we can conclude that the Drude weight for low temperatures behaves as

$$\sigma^{DW}(T \to 0) \sim \frac{1}{\ln(\hbar\Omega/k_B T)^{\bar{\gamma}}}. \tag{32}$$

Actually the effect of finite $\bar{\gamma}$ can even wash the Drude weight out as in the naive Drude model for electric conductivity of metals. Nevertheless, in our specific model, although σ^{DW} is reduced, it is still finite even in the presence of damping for finite T. Moreover, as the ratio $\hbar\Omega/k_B T$ is directly proportional to the number of TLSs in the lowest energy state, it is expected that as the temperature is lowered this number rises, increasing the ability of the particle to lose energy and consequently leading to a smaller value of σ^{DW}.

Now we turn our attention to the behavior of the incoherent part of the optical conductivity, which is given by

$$\sigma^{inc}(\omega) = \sigma_0 \frac{\bar{\gamma}\tanh(\hbar\omega/2k_B T)\Theta(\Omega-\omega)}{2\omega\{\mathcal{Q}^2(\omega,T) + [(\pi\bar{\gamma}/2)\tanh(\hbar\omega/2k_B T)]^2\}}, \tag{33}$$

with

$$\mathcal{Q} = 1 + \frac{4\bar{\gamma}}{\pi}\sum_{n=1}^{\infty} \frac{(2n-1)\arctan[\hbar\Omega/\pi k_B T(2n-1)]}{(2n-1)^2 + (\hbar\omega/\pi k_B T)^2} - \frac{\bar{\gamma}}{2}\tanh\left(\frac{\hbar\omega}{2k_B T}\right)\ln\frac{|\Omega+\omega|}{|\Omega-\omega|}. \tag{34}$$

The presence of the step function in Eq. (33) ensures that $\sigma^{inc}(\omega)$ is exactly zero above the cutoff frequency. Although for frequencies of the order of Ω our approach may provide nonaccurate results, the zero conductivity in the $\omega > \Omega$ region agrees with the fact that all particle transitions between states with energy difference larger than $\hbar\Omega$ are forbidden. This effect is a consequence of having limited the thermal bath phase space by an abrupt cutoff frequency.

In order to discuss the main features of the incoherent part of the optical conductivity given by Eqs. (33) and (34) we begin by calculating the temperature dependence of the dc conductivity $\sigma_{dc}=\sigma^{inc}(\omega=0)$, namely,

$$\frac{\sigma_{dc}(T)}{\sigma_0} = \frac{\hbar\bar{\gamma}}{4k_B T}\left[1 + \frac{4\bar{\gamma}}{\pi}\sum_{n=1}^{\infty}\frac{\arctan[\hbar\Omega/\pi k_B T(2n-1)]}{(2n-1)}\right]^{-2}.$$

The high temperature limit of this expression can be written as

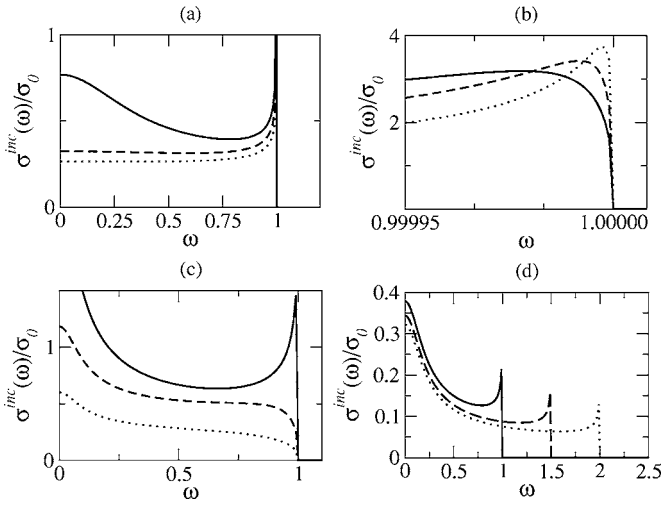

FIG. 3. (a) σ^{inc} as a function of ω for different temperatures with $\bar{\gamma}=0.2$ and $\Omega=1$. The continuous, dashed, and dotted lines correspond to $T=0.09$, $T=0.5$, and $T=2.0$, respectively. (b) Details of $\sigma(\omega)$ near $\omega=\Omega$. (c) σ^{inc} as a function of ω for different coupling strengths. The continuous, dashed, and dotted lines correspond to $\bar{\gamma}=0.4$, $\bar{\gamma}=1.5$, and $\bar{\gamma}=3.5$, respectively, with $T=0.02$ and $\Omega=1$. (d) σ^{inc} vs ω for $\bar{\gamma}=0.2$ and $T=0.05$ for different cutoff frequencies; the continuous, dashed, and dotted lines corresponds to $\Omega=1$, $\Omega=1.5$, and $\Omega=2$, respectively. In all cases the optical conductivity is measured in units of σ_0 and it is assumed $\hbar=k_B=1$.

$$\frac{\sigma_{dc}(T)}{\sigma_0}=\frac{\hbar\bar{\gamma}/4k_BT}{[1+\hbar\bar{\gamma}\Omega/2\pi k_BT]^2},$$

which correctly goes to zero as the temperature increses in agreement with the free particle behavior. The interesting point comes from the divergence at zero temperature. This singular behavior has been observed in classical nonintegrable nonlinear systems where the current correlation decays to zero in the long time limit, but so slowly, that the integral over time, which yields the dc conductivity, diverges.[16] In the present case this result can be understood by realizing that the long time behavior of the damping function (21) involves low frequency modes, but the latter do not have enough spectral weight for the $s=2$ case to make the current decay.

A further understanding of the problem can be achieved after the analysis of Fig. 3, where the frequency dependence of $\sigma^{inc}(\omega)$ is plotted for some particular cases. Notice in Fig. 3(a) that as the temperature increases, the conductivity is reduced in the entire frequency range. This is in agreement with the fact that as one moves toward the limit in which $k_BT\gg\hbar\Omega$, the particle approaches the free behavior and eventually the incoherent conductivity vanishes, see Eqs. (33) and (34), retrieving the free particle result.

Let us now inspect the behavior of $\sigma^{inc}(\omega)$ when $\omega\to\Omega$. Figure 3(b) shows a zoom of Fig. 3(a) for ω around Ω. Near the cutoff frequency the conductivity reaches a maximum and then continuously falls to zero as one approaches Ω from below. This nonmonotonic behavior of the optical conductivity as a function of the frequency can be basically attributed to memory effects of the damping function (21). This effect

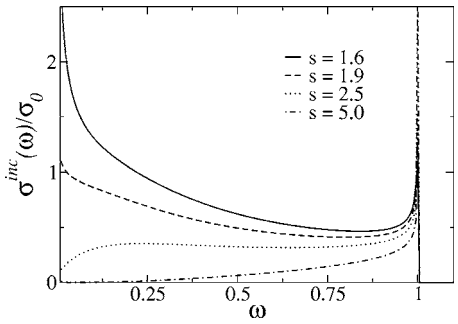

FIG. 4. σ^{inc} as a function of ω—in units of σ_0—for different values of s in the superohmic regime. Notice that as s increases, the value of the σ_{dc} decreases for a given frequency. All graphics were generated assuming $\bar{\gamma}=0.2$, $T=0.09$, $\Omega=1$, and $\hbar=k_B=1$.

is responsible for the dephasing of the different contributions of the bath reaction on the particle. As a matter of fact, if we reanalyze Eq. (33), we observe that the classical impedance $Z(\omega,T)$ of the reservoir (for $\omega<\Omega$) corresponds to

$$Z=\sigma_0^{-1}\left[\frac{2\omega\mathcal{Q}^2(\omega,T)}{\bar{\gamma}\tanh(\hbar\omega/2k_BT)}+\frac{\pi^2\bar{\gamma}\omega}{2}\tanh(\hbar\omega/2k_BT)\right].$$

Although this expression cannot be clearly separated into reactive and resistive contributions, one of the components of the former will be

$$\mathcal{X}(\omega,T)\propto\frac{2\omega\mathcal{Q}^2(\omega,T)}{\bar{\gamma}\tanh(\hbar\omega/2k_BT)},$$

where $\mathcal{Q}(\omega,T)$ is given by Eq. (34). From the definition of $\mathcal{Q}(\omega,T)$, we observe that part of the reaction of the bath over the particle is nothing but a competition of terms with a π phase difference between them, which causes this kind of resonancelike behavior. The effect described above does not appear in the oscillator model, where the bath reacts as a pure resistance due to its memoryless character, and leads to a monotonic behavior of $\sigma^{inc}(\omega)$. It is also expected that as the coupling strength of the particle-reservoir interaction increases, the conductivity will decrease. This effect is illustrated in Fig. 3(c), where it can be seen also that for strong enough coupling the optical conductivity becomes a monotonic function. It remains to mention that for a fixed value of the temperature, an increase in the value of the frequency cutoff leads to a displacement of the conductivity edge to higher frequencies and to a decrease of σ^{inc} in the whole frequency range. This effect is illustrated in Fig. 3(d) and it is a consequence of the higher number of states to scatter the particle, as the value of the cutoff frequency is increased at a given temperature.

All the previous analysis developed for the $s=2$ specific case illustrates to some extent the transport properties of the system in the superohmic regime ($s>1$). However, it is worth mentioning that there are significant differences in the low frequency region of the optical conductivity as one moves from $1<s<2$ to $s>2$ situation—see Fig. 4 for instance. The divergence in the dc conductivity is suppressed

for $s>2$ while it persists for $s<2$. This is again a consequence of the different spectral weights for the low frequency modes as the value of s is changed.

To conclude this part of the analysis we summarize our main findings. In the specific case of $s=2$ the system behaves as a perfect conductor at $T=0$ because of the infinite σ_{dc} conductivity. However, this fact is not reflected in the value of the Drude weight, which goes to zero as T decreases. This contradiction in the classification into metallic or insulator states according to the value of the Drude weight is only apparent. This is so because the current carriers in our approach are not in an eigenstate of the system invalidating the characterization of conductors and insulators in terms of the behavior of σ^{DW}. Another point to be mentioned is the fact that for $s\neq 2$ the dc conductivity, at $T=0$, strongly depends on the s value, see Fig. 4. Finally, above the cutoff Ω, the optical conductivity is always zero at any temperature, independent of the s value.

B. Ohmic case, $s=1$

This case is of particular importance because it allows us to explicitly show the differences with the oscillator model discussed in Refs. 2 and 5. In this specific situation it is useful to notice that

$$ {}_2F_1(1,1,2,-x^2) = \frac{\ln x^2+1}{x^2}. $$

Therefore, the general expression (23) for the Laplace transform of the damping function becomes

$$ \Gamma(z) = \frac{1}{2}\tan\left(\frac{\hbar z}{2k_BT}\right)\ln\left[1+\frac{\Omega^2}{z^2}\right] - \frac{2\hbar z}{\pi^2 k_B T}\sum_{n=1}^{\infty}\frac{\ln\{1+[\hbar\Omega/(2n-1)\pi k_BT]^2\}}{(2n-1)^2-(\hbar z/\pi k_BT)^2}. \quad (35) $$

By substituting Eq. (35) into Eq. (24), we obtain the optical conductivity as a sum of a coherent part given by $\sigma^{DW}(T)\delta(\omega)$, where

$$ \frac{\sigma_0}{\sigma^{DW}} = 1+\frac{\hbar\bar{\gamma}}{k_BT}\left(\sum_{n=1}^{\infty}\frac{\ln\{1+[\hbar\Omega/(2n-1)\pi k_BT]^2\}}{(2n-1)^2}+\frac{1}{2}\right), \quad (36) $$

and an incoherent contribution of the form

$$ \sigma^{inc}(\omega) = \frac{(\bar{\gamma}\pi/2)\tanh(\hbar\omega/2k_BT)\sigma_0\Theta(\Omega-\omega)}{[\bar{\gamma}\pi\tanh(\hbar\omega/2k_BT)/2]^2+\mathcal{R}^2(\omega,T)}, \quad (37) $$

where

$$ \mathcal{R} = \omega+\frac{\bar{\gamma}}{2}\tanh\left(\frac{\hbar\omega}{2k_BT}\right)\ln\left(\frac{\Omega^2-\omega^2}{\omega^2}\right) - \frac{2\bar{\gamma}\hbar\omega}{\pi^2 k_BT}\sum_{n=1}^{\infty}\frac{\ln\{1+[\hbar\Omega/(2n-1)\pi k_BT]^2\}}{(2n-1)^2+(\hbar\omega/\pi k_BT)^2}. \quad (38) $$

Once again the Drude weight cannot be obtained exactly for all temperatures, except for $k_BT\gg\hbar\Omega$. In this limit we find

$$ \sigma^{DW}(T) = \sigma_0\left[1+\frac{\pi^2\bar{\gamma}}{96\Omega}\left(\frac{\hbar\Omega}{k_BT}\right)^3\right]^{-1}, \quad (39) $$

which correctly reproduces the expected free particle conductivity in the infinite temperature regime, where the incoherent contribution goes to zero [see Eqs. (37) and (38)]. If one compares Eqs. (28) and (39), one realizes that for the same temperature the Drude weight in the $s=2$ case is lower than the $s=1$ case. This is nothing but the effect of the stronger coupling between the particle and the reservoir modes as value of s—characterizing the thermal bath—is increased.

The low temperature properties of the Drude weight can be derived from Eq. (36) by considering a value of $n=\bar{n}$ such that $\hbar\Omega/k_BT\gg\bar{n}$. In this case the sum involved in Eq. (36) can be written approximately as

$$ \mathcal{S} = \ln\left(\frac{\hbar\Omega}{k_BT}\right)\sum_{n=1}^{\bar{n}}\frac{1}{(2n-1)^2}-\sum_{n=1}^{\bar{n}}\frac{\ln\pi(2n-1)}{(2n-1)^2} + \sum_{n=\bar{n}}^{\infty}\frac{\ln\{1+[\hbar\Omega/(2n-1)\pi k_BT]^2\}}{(2n-1)^2}. \quad (40) $$

Notice that for $T\to 0$ the value of $\bar{n}$ goes to infinity and therefore the first term in the right-hand side (rhs) of Eq. (40) dominates the sum. Substituting this result into Eq. (36) we obtain that for low temperatures the Drude weight goes to zero as

$$ \sigma^{DW}(T\to 0)\propto\frac{k_BT}{\hbar\bar{\gamma}\ln[\hbar\Omega/k_BT]}. \quad (41) $$

This expression correctly reproduces the well-known result for the oscillator model,[5] namely, there is no coherent contribution to the conductivity when Ω goes to infinity. This result could have been foreseen from the analysis of the particle dynamics [see Eq. (21) for $s=1$ and $T\to 0$]. It should be stressed that for $s=1$ σ^{DW} goes to zero faster than for $s=2$ [see Eq. (32)], as a consequence of the stronger interaction of the particle with the low energy modes.

After having examined the temperature dependence of the Drude weight for ohmic dissipation in the analytically accessible limits, we proceed to a numerical evaluation of Eq. (36). Figure 5(a) shows the behavior of the Drude weight as a function of temperature for different coupling strength values. Observe that for any given temperature σ^{DW} decreases as the interaction strength becomes stronger. Indeed, for stronger interactions the momentum transferred to the reservoir is larger and consequently the conductivity is reduced. This also implies that the free particle behavior will be reached at higher temperatures as $\bar{\gamma}$ increases.

Our next step is the analysis of the incoherent part of the optical conductivity. The first point to be mentioned is the infinite dc conductivity of the system at any finite temperature. This result is obtained taking the limit of zero frequency in the expressions (37) and (38) and can be explained by the fact that the dc conductivity is determined by the low frequency modes in the damping function (21). We have plotted in Fig. 5(b) σ^{inc} vs ω for different temperatures with a finite cutoff frequency $\Omega=1$. The forbidden particle transitions involving energy exchange above $\hbar\Omega$ leads to zero conductiv-

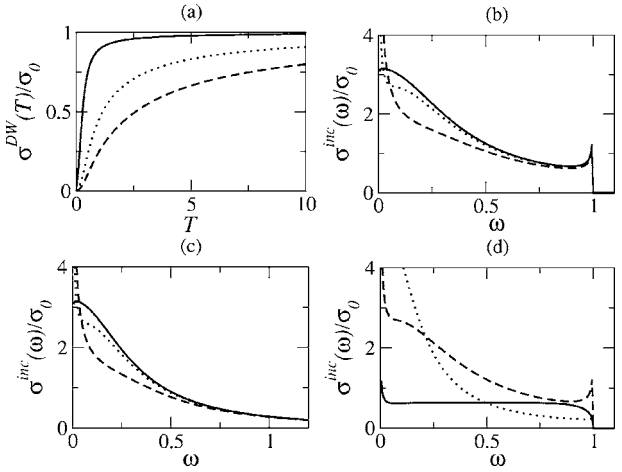

FIG. 5. (a) σ^{DW} as a function of T for different coupling strength with $\Omega=1$. The continuous, dotted, and dashed lines correspond to $\bar{\gamma}=0.2$, $\bar{\gamma}=2$, and $\bar{\gamma}=5$, respectively. (b) $\sigma(\omega,T)$ vs ω for different temperatures with $\bar{\gamma}=0.2$ and $\Omega=1$. The continuous, dotted, and dashed lines correspond to $T=0.001$, $T=0.02$, and $T=0.09$, respectively. (c) The same as (b) assuming $\Omega=100$. (d) σ^{inc} vs ω for $\Omega=1$ and $T=0.02$ for different coupling strength, the continuous, dashed, and dotted lines corresponds to $\bar{\gamma}=1$, $\bar{\gamma}=0.2$, and $\bar{\gamma}=0.09$, respectively. In all cases the conductivity is measured in units of σ_0 and it is assumed $\hbar=k_B=1$.

ity for $\omega>\Omega$, as already obtained in the $s=2$ case. One may also notice that as the temperature increases the conductivity grows for small values of ω. This can be understood by recalling that as the temperature rises, the particle-reservoir interaction—which can actually change the particle momentum—is less effective for the low energy modes and consequently the conductivity also rises for such frequencies. It should be also mentioned that as the temperature is lowered, $\sigma^{inc}(\omega)$ acquires a Lorentzian form. This behavior becomes evident in Fig. 5(c), in which we considered $\Omega=100$. At lower temperatures one approaches the oscillator model. Indeed, taking the limits $\Omega\to\infty$ and $T\to 0$, we obtain

$$\sigma^{inc}(\omega)=\frac{\pi\bar{\gamma}/2}{\omega^2+(\pi\bar{\gamma}/2)^2}\sigma_0,$$

which is the well-known result for the oscillator model. Finally, Fig. 5(d) shows the effect of varying the coupling strength. The main feature to be observed is the reduction of the conductivity as $\bar{\gamma}$ increases, consistent with the fact that it is then easier for the particle to transfer momentum to the reservoir.

C. Subohmic case, $s=0$

Another interesting result, which differs considerably from the cases already discussed, arises when $s=0$. In this case, the hypergeometric function reads

$${}_2F_1(1,1/2,3/2,-x^2)=\frac{\arctan x}{x}$$

and the Laplace transform of the damping function given by Eq. (23) acquires the form

$$\Gamma(z)=\frac{4k_BTz}{\hbar}\sum_{n=1}^{\infty}\frac{1}{\lambda_n^2-z^2}\left[\frac{\arctan(\Omega/z)}{z}-\frac{\arctan(\Omega/\lambda_n)}{\lambda_n}\right], \tag{42}$$

where we have used that $\lambda_n=(2n-1)k_BT\pi/\hbar$ with n integer.

Substituting now Eq. (42) into Eq. (24), we obtain an expression for the optical conductivity which has zero Drude weight at all temperatures and an incoherent part of the form

$$\sigma^{inc}(\omega)=\sigma_0\frac{2\bar{\gamma}\omega\tanh(\hbar\omega/2k_BT)\Theta(\Omega-\omega)}{\mathcal{G}^2(\omega,T)+[\pi\bar{\gamma}\tanh(\hbar\omega/2k_BT)]^2}, \tag{43}$$

with

$$\mathcal{G}=2\omega^2-\frac{8\hbar^2\bar{\gamma}\omega^2}{\pi^3k^2T^2}\sum_{n=1}^{\infty}\frac{\arctan(\hbar\Omega/N\pi k_BT)}{N[N^2+(\hbar\omega/\pi k_BT)^2]}+\bar{\gamma}\tanh\left(\frac{\hbar\omega}{2k_BT}\right)\ln\frac{|\Omega-\omega|}{|\Omega+\omega|}. \tag{44}$$

The dc conductivity, obtained by taking the $\omega\to 0$ limit in Eqs. (43) and (44), may be written as $\sigma_{dc}/\sigma_0=4k_BT/\pi^2\hbar\bar{\gamma}$. From this result we conclude that the system behaves as an insulator with zero dc conductivity at $T=0$.

Inspection of Eq. (43) yields that the incoherent part of the conductivity is finite only below the cutoff frequency, just as in the cases discussed previously. Another important feature is the way in which one may recover the free particle behavior. In order to analyze this limit it should be noticed that at high temperatures Eqs. (43) and (44) may be written as

$$\sigma^{inc}(\omega)=\frac{e^2}{M}\frac{\zeta}{\omega^2+\zeta^2}, \tag{45}$$

where $\zeta=\pi\hbar\bar{\gamma}/4k_BT$. In the limit $\zeta\to 0$, which corresponds to infinite temperature or zero coupling strength, Eq. (45) goes to $(\pi e^2/M)\delta(\omega)$, correctly reproducing the optical conductivity of a free particle.

The general behavior of $\sigma^{inc}(\omega)$ is displayed in Fig. 6 for different values of temperature, coupling strength, and cutoff frequency. Figure 6(a) shows that as the temperature increases, one approaches the frequency dependence given by Eq. (45), which has a maximum at $\omega=0$. In this regime, the classical impedance of the reservoir is purely resistive, analogous to the oscillator-bath model. However, as the temperature decreases, the value of $Z(\omega)$ is determined by a competition between terms completely out of phase, see Eq. (44), reaching the maximum value for $\omega\neq 0$. For $T\to 0$, the frequency at which the conductivity exhibits a maximum becomes closer to the cutoff frequency, characterizing an extreme non-Drude behavior. As one approaches Ω from below, no matter the value of the temperature, the conductivity smoothly falls to zero. This effect, which is related to the lack of available states in the reservoir to scatter the particle, is shown in Fig. 6(b). It is also worth mentioning the small variations of the maximum conductivity as the cutoff frequency is changed, as illustrated in Fig. 6(c). Finally, Fig. 6(d) shows the effect of varying the value of the coupling strength $\bar{\gamma}$ for a given temperature and cutoff frequency. An

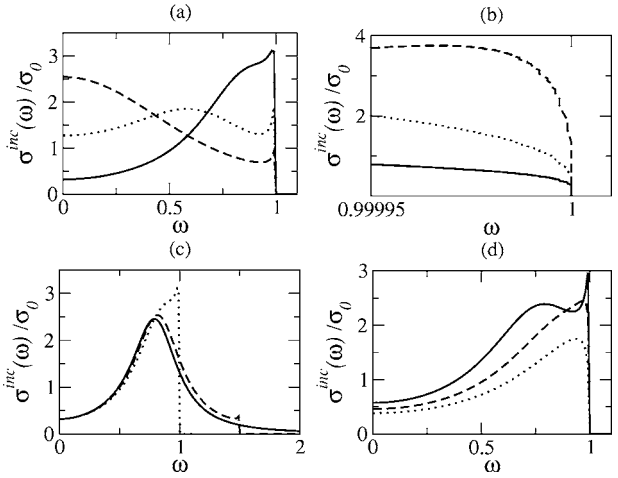

FIG. 6. (a) Incoherent contribution to the optical conductivity for different temperatures with $\bar{\gamma}=0.2$ and $\Omega=1$. The continuous, dotted, and dashed lines correspond to $T=0.05$, $T=0.2$, and $T=0.4$, respectively. (b) Detail of (a) near the cutoff frequency. (c) σ^{inc} vs ω for different values of Ω. The continuous, dashed, and dotted lines corresponds to $\Omega=100$, $\Omega=1.5$, and $\Omega=1$, respectively, in all cases $\bar{\gamma}=0.2$ and $T=0.05$. (d) σ^{inc} vs ω for different values of the coupling strength. The continuous, dashed, and dotted lines corresponds to $\bar{\gamma}=0.2$, $\bar{\gamma}=0.25$, and $\bar{\gamma}=0.3$, respectively, with $\Omega=1$ and $T=0.09$. In all cases the optical conductivity is measured in units of σ_0 and it is assumed $\hbar=k_B=1$.

increase in the interaction strength leads to a reduction of the conductivity. This is an expected result because for larger values of $\bar{\gamma}$, the particle can transfer momentum to the reservoir in an effective way, and as a consequence, the conductivity is reduced.

At this point we can conclude the $s=0$ analysis pointing out that in this situation the conductivity is always incoherent and nonzero just below the cutoff frequency with a dc value that vanishes as T goes to zero. In order to verify if those features are common to the entire subohmic regime, we have numerically evaluated the combined Eqs. (42) and (24) for different values of $s<1$, see Fig. 7(a). As it can be observed, the general behavior of the conductivity resembles the $s=0$ case (see Fig. 6), except in the low frequency region. This fundamental difference is illustrated in Fig. 7(b) showing that σ^{inc} is singular at $\omega=0$, although our numerical calculation indicates that the Drude weight remains zero at any finite temperature and value of s. In order to investigate in more detail the general behavior of σ^{inc} in the low frequency region, it is useful to notice that near $\omega=0$ the optical conductivity does not depend on the value of the cutoff frequency, see Fig. 7(c). Therefore, we may simply take the limit $\Omega\to\infty$ in the Laplace transform of the damping function given by Eq. (23) and obtain an expression for $\Gamma(z)$ for any $0<s<1$, namely,

$$\Gamma(z)=\frac{2\pi k_B T z}{\hbar\cos(\pi s/2)}\sum_{n=1}^{\infty}\frac{z^{s-1}-\lambda_n^{s-1}}{\lambda_n^2-z^2}. \tag{46}$$

Substituting the expression above in Eq. (24) we obtain the optical conductivity, which has a zero Drude weight, besides an incoherent contribution given by

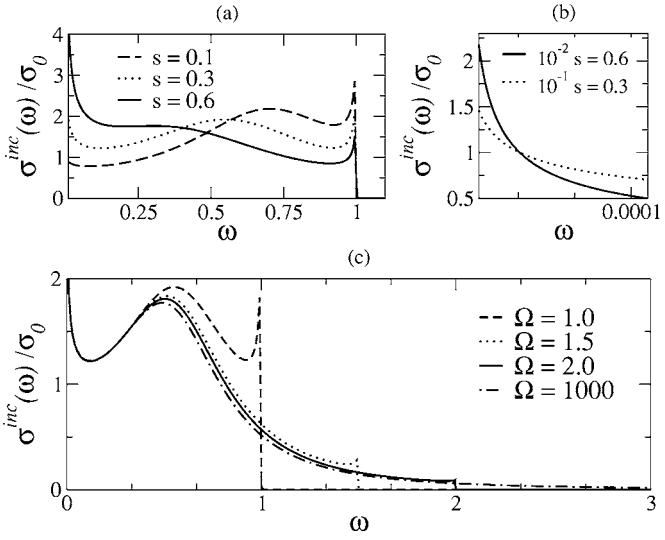

FIG. 7. (a) Incoherent contribution to the optical conductivity in the subohmic regime, in all cases it was assumed $\bar{\gamma}=0.2$, $T=0.09$, and $\Omega=1$. (b) Detailed form of the conductivity in (a) near $\omega=0$ for $s=0.6$ and $s=0.3$. (c) σ^{inc} vs ω for different values of Ω, in all cases $T=0.09$, $\bar{\gamma}=0.2$, and $s=0.3$. The optical conductivity is always measured in units of σ_0 and it is assumed $\hbar=k_B=1$.

$$\frac{\sigma^{inc}(\omega)}{\sigma_0}=\frac{2\bar{\gamma}\omega^{s-3}\tanh(\hbar\omega/2k_BT)}{4\mathcal{K}^2(\omega,s)+[\pi\bar{\gamma}\omega^{s-1}\tanh(\hbar\omega/2k_BT)]^2}, \tag{47}$$

where

$$\mathcal{K}=1+\frac{\pi\bar{\gamma}}{2}\tan(s\pi/2)\omega^{s-2}\tanh(\hbar\omega/2k_BT)$$
$$-\frac{2\bar{\gamma}(\pi k_BT)^2}{\hbar^2\cos(s\pi/2)}\sum_{n=1}^{\infty}\frac{(2n-1)^{s-1}}{(2n-1)^2+(\hbar\omega/2k_BT)^2}. \tag{48}$$

This result is in complete agreement with the previous numerical analysis for finite cutoff frequency and promptly allows us to derive the way in which the conductivity diverges as one approaches $\omega=0$,

$$\frac{\sigma^{inc}(\omega\sim 0)}{\sigma_0}=\frac{4k_BT\cos^2(\pi s/2)}{\pi^2\hbar\bar{\gamma}}\omega^{-s}.$$

It is worth mentioning that this expression is also valid for the $s=0$ case [see Eq. (42), for instance], correctly reproducing the finite $\sigma_{dc}(T)$ value already found.

With the analysis of the $\Omega\to\infty$ limit we conclude that the finite dc conductivity obtained for the $s=0$ case is an exception within the subohmic regime, in which the dc conductivity is, in general, divergent. This discussion summarizes our main findings in the study of the optical conductivity for cases in which $0\leqslant s<1$.

V. CONCLUSIONS

We have studied the transport properties of noninteracting particles coupled to a set of two-level systems described by a temperature-dependent spectral function. Our approach was

TABLE I. Summary of results.

	σ_{dc}	$\sigma^{DW}_{T\to 0}$	$\sigma^{DW}_{T\to\infty}$	$\sigma^{inc}_{T\to 0}$	$\sigma^{inc}_{T\to\infty}$
Superohmic	Diverges for $T\to 0$[a]	zero	σ_0	Anomalous insulator—non-Drude	zero
Ohmic	Diverges for finite T[b]	zero	σ_0	Insulator—Lorentzian form[b]	zero
Subohmic	Diverges for finite T[c]	⋯	⋯	Perfect insulator—non-Drude	$\sigma_0\delta(\omega)$

[a]For $s\leqslant 2$, in other cases it is finite.
[b]For $\Omega\to\infty$ reproduces the oscillator results.
[c]Except in the $s=0$ case, where the σ_{dc} goes to zero.

based on the Feynman-Vernon functional-integral formalism which allows us to trace out the two-level system coordinates and obtain an effective equation of motion for the particle in terms of the phenomenological TLSs spectral function.

The evaluation of the transport properties were performed considering different values of the power s of the generic spectral function, which is proportional to ω^s. Two different regimes were found; the superohmic ($s>1$) and ohmic ($s=1$) in which the optical conductivity has both, coherent and incoherent contributions, and the subohmic ($s<1$) where the conductivity is strictly incoherent. In the first case the Drude weight goes to zero as the temperature decreases in a logarithmic fashion and the incoherent part shows a strong non-Drude behavior with a divergent dc conductivity for $T=0$, except for the ohmic case in which the zero temperature dc conductivity is finite. In the entire subohmic regime, the Drude weight is always zero at all temperatures. In contrast, the dc conductivity is only finite in the $s=0$ specific case, going linearly to zero as the temperature decreases, whereas in general it is divergent at all temperatures. It should be mentioned that in this regime, the general behavior of $\sigma(\omega)$ is strongly non-Drude, with the highest conductivity arising at finite values of ω. All these properties strongly differ from the simple behavior induced by an oscillator thermal bath on a system of noninteracting particles. The latter exhibits no temperature dependence and zero Drude weight with a finite dc conductivity. All this results are summarized in Table I. Concerning the limitation of the approach employed here, it is important to stress that it is accurate for long times (or low frequencies) compared with the response time of the system, which is basically Ω^{-1}. Therefore in all cases where the cutoff frequency was assumed to be finite, the values of the optical conductivity near $\omega=\Omega$ should be interpreted carefully.

Finally, as the model analyzed here could be relevant for the study of the dynamics of a particle in the presence of a distribution of locally quartic plus quadratic potentials, we expect it may contribute to the understanding of the transport properties of low dimensional systems at low temperatures, where the physics is often dominated by defects and impurities.

ACKNOWLEDGMENTS

A.V.F. kindly acknowledges the financial support from Fundação de Amparo à Pesquisa do Estado de São Paulo (FAPESP) at the Universidade Estadual de Campinas, and A.O.C. acknowledges the partial support from Conselho Nacional de Desenvolvimento Científico e Tecnológico (CNPq). We are grateful to Milena Grifoni for a critical reading of the manuscript and to the Swiss National Foundation for Scientific Research, Grant No. 620-62868.00, which allowed for the establishment of this collaboration.

APPENDIX

In order to calculate the Laplace transform of $\Gamma(t)$ we will use the expansion[17]

$$\tanh\left(\frac{\pi x}{2}\right)=\frac{4x}{\pi}\sum_{n=1}^{\infty}\frac{1}{(2n-1)^2+x^2},$$

which allows us to rewrite $\Gamma(z)$ as

$$\Gamma(z)=\frac{4k_BTz}{\hbar}\sum_{n=0}^{\infty}\mathbb{I}(n,\Omega), \tag{A1}$$

where

$$\mathbb{I}(n,\Omega)=\int_0^{\Omega}\frac{\omega'^s d\omega'}{(\omega'^2+z^2)(\omega'^2+\lambda_n^2)},$$

with $\lambda_n=(2n-1)\pi k_BT/\hbar$ and $n\in\mathbb{N}$. This integral can be split into two terms,

$$\mathbb{I}=\frac{1}{z^2-\lambda_n^2}\left[z^2\int_0^{\Omega}\frac{\omega'^{s-2}d\omega'}{(\omega'^2+z^2)}-\lambda_n^2\int_0^{\Omega}\frac{\omega'^{s-2}d\omega'}{(\omega'^2+\lambda_n^2)}\right].$$

The new integrals are easily performed, yielding

$$\int_0^{\Omega}\frac{\omega'^{s-2}d\omega'}{(\omega'^2+\nu^2)}=\frac{\Omega^{s-1}}{\nu^2}\sum_{m=0}^{\infty}\frac{(-1)^m}{2m+s-1}\left(\frac{\Omega}{\nu}\right)^{2m}.$$

We now rewrite the expression for $\mathbb{I}(n,\Omega)$ as

$$\mathbb{I}(n,\Omega)=\frac{\Omega^{s+1}}{(\lambda_n^2-z^2)}\left[\frac{1}{z^2}\sum_{m=1}^{\infty}\frac{(-1)^{m-1}}{2m+s-1}\left(\frac{\Omega}{z}\right)^{2m-2}-\frac{1}{\lambda_n^2}\sum_{m=1}^{\infty}\frac{(-1)^{m-1}}{2m+s-1}\left(\frac{\Omega}{\lambda_n}\right)^{2m-2}\right]. \tag{A2}$$

Substituting this equation into Eq. (A1) and expressing the sums involved in Eq. (A2) in terms of the hypergeometric functions we obtain

$$\Gamma(z) = \frac{4k_B T z}{\hbar(s+1)} \sum_{n=1}^{\infty} \frac{\Omega^{s+1}}{\lambda_n^2 - z^2} \left[\frac{{}_2F_1[1,(1+s)/2,(3+s)/2,-\Omega^2/z^2]}{z^2} - \frac{{}_2F_1[1,(1+s)/2,(3+s)/2,-\Omega^2/{\lambda_n}^2]}{{\lambda_n}^2} \right]. \tag{A3}$$

By performing the sum in the first term of Eq. (A3) and introducing the notation ${}_2F_1[1,(1+s)/2,(3+s)/2,x]=F(s,x)$, we finally obtain Eq. (23).

[1] R. P. Feynman and F. L. Vernon, Ann. Phys. **24**, 118 (1963).
[2] A. O. Caldeira and A. J. Leggett, Physica A **121**, 587 (1983).
[3] A. J. Leggett *et al.*, Rev. Mod. Phys. **59**, 1 (1987).
[4] N. V. Prokof'ev and P. C. E. Stamp, Rep. Prog. Phys. **63**, 669 (2000).
[5] A. O. Caldeira and A. J. Leggett, Ann. Phys. (N.Y.) **149**, 347 (1983).
[6] P. Hedegard and A. O. Caldeira, Phys. Scr. **35**, 609 (1987).
[7] A. H. Castro Neto and A. O. Caldeira, Phys. Rev. E **48**, 4037 (1993).
[8] A. Villares Ferrer and A. O. Caldeira, Phys. Rev. B **61**, 2755 (2000).
[9] A. Villares Ferrer and A. O. Caldeira, Phys. Rev. B **64**, 104425 (2001).
[10] See T. Kato and M. Imada, J. Phys. Soc. Jpn. **67**, 2828 (1998), and references therein.
[11] A. T. Dorsey, M. P. A. Fisher, and M. S. Wartak, Phys. Rev. A **33**, 1117 (1986).
[12] A. O. Caldeira, A. H. Castro Neto, and T. Oliveira de Carvalho, Phys. Rev. B **48**, 13974 (1993).
[13] N. Makri, J. Phys. Chem. B **103**, 2823 (1999).
[14] A general discussion about how nontrivial spectral functions can be decomposed in the form used here can be found in U. Weiss, *Quantum Dissipative Systems*, 2nd ed., Series in Modern Condensed Matter Physics Vol. 10 (World Scientific, Singapore, 1999).
[15] P. M. V. B. Barone and A. O. Caldeira, Phys. Rev. A **43**, 57 (1991).
[16] X. Zotos and P. Prelovsek, in *Strong Interactions in Low Dimensions*, edited by D. Baeriswyl and L. Degiorgi (Kluwer Academic, Dordrecht, 2004).
[17] I. S. Gradshteyn and I. M. Ryzhik, *Table of Integrals and Products* (Academic, New York, 2000).